

A Bio-Inspired Chaos Sensor Based on the Perceptron Neural Network: Concept and Application for Computational Neuroscience

Andrei Velichko^{1,*}, Petr Boriskov¹, Maksim Belyaev¹ and Vadim Putrolaynen¹

¹ Institute of Physics and Technology, Petrozavodsk State University, 33 Lenin str., 185910, Petrozavodsk, Russia

* Correspondence: velichko@petrsu.ru;

Abstract: The study presents a bio-inspired chaos sensor based on the perceptron neural network. After training, the sensor on perceptron, having 50 neurons in the hidden layer and 1 neuron at the output, approximates the fuzzy entropy of short time series with high accuracy with a determination coefficient $R^2 \sim 0.9$. The Hindmarsh-Rose spike model was used to generate time series of spike intervals, and datasets for training and testing the perceptron. The selection of the hyperparameters of the perceptron model and the estimation of the sensor accuracy were performed using the K-block cross-validation method. Even for a hidden layer with 1 neuron, the model approximates the fuzzy entropy with good results and the metric $R^2 \sim 0.5 - 0.8$. In a simplified model with 1 neuron and equal weights in the first layer, the principle of approximation is based on the linear transformation of the average value of the time series into the entropy value. The bio-inspired chaos sensor model based on an ensemble of neurons is able to dynamically track the chaotic behavior of a spiked biosystem and transmit this information to other parts of the biosystem for further processing. The study will be useful for specialists in the field of computational neuroscience.

Keywords: chaos; chaos sensor; neural network; perceptron; biosensor; entropy; bio-inspired; computational neuroscience; Hindmarsh–Rose neuron model; fuzzy entropy

1. Introduction

Numerous studies in the field of neurophysiology and biophysics over the past 40 years showed that chaotic dynamics is an inherent property of the brain. Neuroscientists are interested in the role of chaos in cognition and the use of chaos in artificial intelligence applications based on neuromorphic concepts. The chaos is important for increasing the sensory sensitivity of cognitive processes [1–7]. For example, the sensory neuronal systems of crayfish and paddlefish use the background noise to detect subtle movements in the water made by predators and victims [1]. Another study of the central nervous system [2] demonstrated that the efficient search for food using memory regions of the olfactory bulb of rabbits is reflected by the chaotic dynamics of electroencephalography (EEG) to. Van der Groen et al. [4] investigated the effect of stochastic resonance on cognitive activity in the brain. The random stimulation of the visual cortex with an optimal noise level can be used as a non-invasive method to improve the accuracy of perceptual decisions. Diagnosis of chaotic and regular states, especially in physiology and medicine, can be of great practical importance. For example, some medical studies consider normal dynamics of health as ordered and regular, while many pathologies are deemed as bifurcations into chaos [8–10]. In that regard, the ventricular fibrillation, an arrhythmia, most often associated with sudden death, is a turbulent process (cardiac chaos), which may be the result of the mechanism of subharmonic bifurcation (period doubling) [9]. On the other hand, a

mild form of ECG chaos may indicate congestive heart failure [11]. The study of the orderliness of the functioning of ensembles of brain neurons by measuring electroencephalograms makes it possible to: identify pathological conditions (neurodegenerative diseases, epilepsy) [12–14]; determine the level of concentration and mental fatigue [15–17]; evaluate the emotional state [18,19]; to produce biometric identification of a person [20,21].

Although scientists are interested in detecting chaos in biological systems to identify pathological conditions, and its influence on the dynamics of bioprocesses, a question may arise: *Can a biosystem itself evaluate the randomness of signals?* A possible answer to this question could be the presentation of a bio-inspired model of the chaos sensor that originates the goal for this study. The paper proposes a bio-inspired tool for assessing chaos based on a multilayer perceptron (Figure 1). The question of whether an ensemble of neurons with a similar function actually exists in real life may be a topic for future research by neurophysiologists.

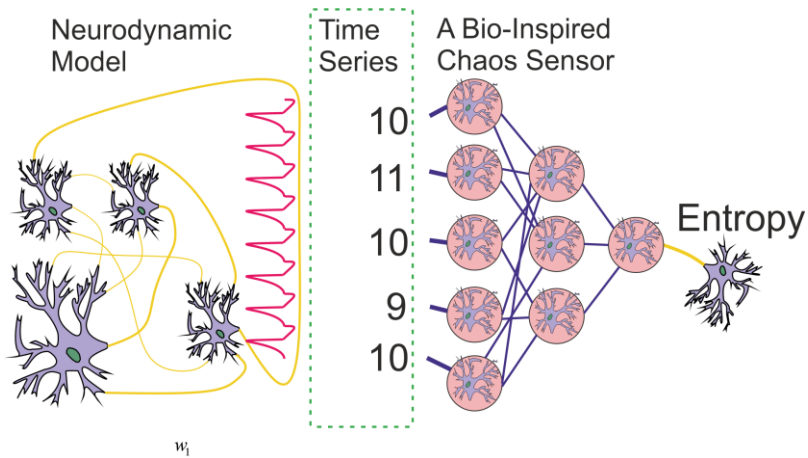


Figure 1. The concept of a chaos sensor based on a perceptron, where a spike signal is input as a time series of periods, and the signal entropy is estimated at the output neuron.

The central (cortical) nervous system (CNS) of the brain is highly heterogeneous. In fact, the neurons are weakly connected to each other, and each of them is directly affected by less than 3% of the surrounding neurons [22]. Moreover, neurons are individual and highly recurrent, that is, they have feedback through the neurons of the environment [23]. The CNS weakly resembles an artificial neural network (ANN) [24], where neuron nodes are functionally equal and each neuron receives a signal from all neurons of the previous layer.

In 1986, Rumelhart, McClelland and their research group introduced the term connectionism [25], which meant a set of algorithms and models with parallel distributed data processing. The concept of connectionism imitates the basic computational properties of groups of real neurons found in the central nervous system using small networks modeling of abstract units [26–28]. However, the first classical example of such small systems, proposed by Rosenblatt [29] long before the work of Rumelhart and McClelland, is the perceptron, the simplest neural network of direct propagation, consisting of separate layers with one output neuron, which linearly separates (classifies) information into two categories. The Rosenblatt's perceptron, consisting of only one (hidden) layer, played an outstanding role in the development of neural technologies. The first ANN developments and the main learning method - the error correction method, known as backpropagation method, were based on Rosenblatt's perceptron [30]. Perceptrons are the building blocks of more complex ANNs [24].

In this paper, we propose the concept of a chaos sensor based on a perceptron. The concept of the sensor is presented in Figure 1. The neurodynamic model generates a spike

signal, and the sensor evaluates its irregularity as an entropy value. The chaos sensor evaluates the regularity of the spike oscillogram from a time series of periods between spikes. The time series is input to the perceptron, and the entropy value is calculated at the output.

For the chaos studies, a reliable method for chaos detection is the key. The main characteristic of chaos is entropy - an additive physical quantity as a measure of the possible states of a system, introduced into the methodology of statistical physics and thermodynamics since the middle of the 19th century. In the 20th century, due to the significant use of the entropy concept in other areas of the natural sciences, including biology, mathematicians proposed numerous variations of this characteristic. A number of entropy indicators and calculation algorithms have appeared for objects with different stochastic and chaotic properties. Among the most known are Shannon entropy [18], sample entropy (SampEn) [19], permutation entropy (PermEn) [20], fuzzy entropy (FuzzyEn) [31], cosine similarity entropy [32], phase entropy [33], singular value decomposition entropy (SvdEn) [34]. The search for new chaos estimation algorithms includes, for example, Neural Network Entropy (NNetEn) [35–37], which is based on the classification of special datasets in relation to the entropy of the time series recorded in the reservoir of the neural network. NNetEn does not take into account probability distribution functions.

FuzzyEn method for estimating the chaos, used in this study, has a number of adjustable parameters, a high calculation speed, and good sensitivity when using short time series.

The possibility of approximating entropy using machine learning regression methods was demonstrated by Velichko et al. [38]. The entropies of SvdEn, PermEn, SampEn and NNetEn were used in the study and the gradient boosting algorithm was recognized as the best regression method. The results of the study were used to accelerate the calculation of 2D image entropy in remote sensing.

Among the neurodynamic models with chaotic dynamics, chaotic 3D models of Hodgkins-Huxley [39], Hindmarsh-Rose [40], modified 2D models of Fitzhugh-Nagumo [41] and Izhikevich [42] can be distinguished.

The Hindmarsh-Rose (HR) system is one of the popular spike models in describing real biological neurons. It appeared as analysis of the Hodgkin-Huxley equations, represented a 2D analog of the Fitzhugh-Nagumo neuron, and allowed to observe long intervals between spike sequences [43]. Later, additional equation was added to the system of equations [8].

One of the applications of the HR model is to simulate the interaction of real neurons in various network architectures. In [44], the influence of the coupling strength and driving current on the behavior of HR neurons in a ring network is studied. In another network with the “all with all” architecture, HR model helped to establish that the difference between the incoming and outgoing current plays a decisive role in the activity of neurons, and this finding can be used to explain the mechanism of short-term memory generation [45]. Various synchronization effects in networks of HR neurons have been investigated [9,46,47]. In addition to the usual (tonic) oscillation mode, the HR model describes the burst activity of neurons, when tonic oscillations alternate with rest states. In addition, in the HR model, chaos is observed at the moment of transition between simple tonic and bursting modes, and can be explained by the theory of homoclinic bifurcations of co-dimension two, which are typical for fast-slow systems [10]. A feature of such bifurcations is the doubling of the periods of both periodic and homoclinic orbits [48].

In this study, we present two models of the chaos sensor. The first model estimates the irregularity of time series through the calculation of FuzzyEn (Sensor on FuzzyEn - (SFU)). The second model estimates (approximates) the degree of chaos by a multilayer perceptron (Sensor on Perceptron - (SPE)), trained on the results of the SFU model. The goal is to create the SPE model, which results, after training the perceptron, would match with the SFU model on R^2 metric in the best possible way. The time series databases for training and testing were created using the Hindmarsh-Rose spike model and the SFU

model. The study reviews the following questions. What is the length of the time series that must be fed to the sensor input in order to calculate the entropy with a given accuracy for the SFU model? What are the optimal FuzzyEn parameters for maximum sensitivity of SFU and SPE sensors. What perceptron parameters are optimal for approximating the entropy function? How does the accuracy of the SPE model approximation depend on the time series normalization method? What is the principle of approximating entropy using a perceptron?

The contributions of the study include:

- Optimal FuzzyEn parameters were determined, allowing to reach maximum sensitivity of the chaos sensor for SFU and SPE models;
- Results indicate that the sensitivity of the SFU sensor increases linearly with the time series length. The relative measurement error for ultrashort time series of length $NL = 20$ elements does not exceed 30%. The relative measurement error for $NL = 50$ does not exceed 11%. The SPE model has similar parameters for $NL = 50$, and, in the averaging mode, the relative error does not exceed 4%.
- Time series databases for training and testing the perceptron model based on the Hindmarsh-Rose spike model and FuzzyEn were created.
- A bio-inspired model of a chaos sensor based on a multilayer perceptron, approximating FuzzyEn, is proposed.
- Results demonstrate that the use of the time series normalization procedure significantly improves the accuracy of the FuzzyEn approximation.
- The proposed perceptron model with 1 neuron in the hidden layer reaches high degree of similarity between SFU and SPE models with an accuracy in the range $R^2 \sim 0.5 - 0.8$, depending on the combination of databases.
- The proposed perceptron model with 50 neurons in the hidden layer reaches an extremely high degree of similarity between SFU and SPE models with an accuracy of $R^2 \sim 0.9$.
- A method for increasing the sensitivity of the sensor through the procedure of averaging the measurement results is proposed.
- Results demonstrate that in the simplified SPE model with 1 neuron and equal weights in the first layer, the principle of entropy approximation is based on a linear transformation of the average value of the time series. In a trained perceptron with 50 neurons, the approximation principle is much more complex.

The rest of the paper is organized as follows. In Section 2, the perceptron model, techniques for modeling the Hindmarsh-Rose system, generating time series, creating databases, calculating and approximating entropy are described. Section 3 is dedicated to numerical results for SFU and SPE models. Section 4 discusses research results and outlines directions for future research. The conclusion is given in Section 5.

2. Materials and Methods

2.1. Perceptron model

The model of the perceptron used as a chaos sensor is shown in Figure 2. The SPE model has one hidden layer, and the output is represented by one neuron with a linear activation function $f(z) = z$, where z is the weighted sum at the input of the neuron. The number of inputs corresponds to the number of elements of the time series NL . In this paper, we consider a model with $NL = 50$. The number of neurons in the hidden layer NH had three gradations $NH = 1, 50$ and 150 with a sigmoid activation function $f(z) = 1/(1+\exp(-z))$. Figure 2a shows a perceptron model with one neuron in the hidden layer $NH = 1$, and Figure 2b shows a model with $NH = 50$ neurons in the hidden layer.

A linear activation function is used on the output neuron, since this approach is most common in regression models, and is effective for approximating the entropy of a time series.

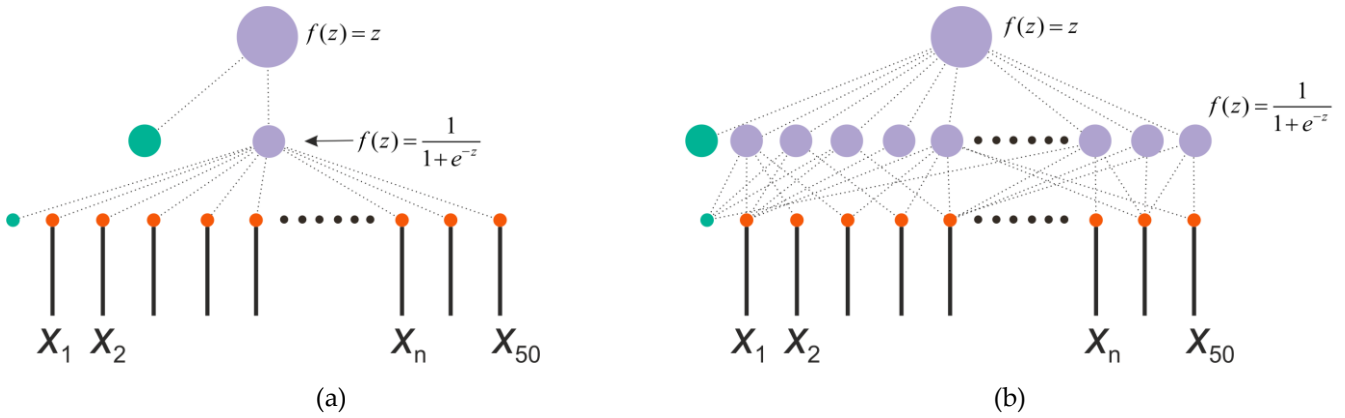


Figure 2. Perceptron model with the number of neurons in the hidden layer $NH = 1$ (a) and $NH = 50$ (b). The figure shows the structure of a perceptron used as a chaos sensor with a different number of neurons in the hidden layer and one output neuron. The input is a time series x_n . The figure shows the activation functions of neurons.

2.2. Modeling the Hindmarsh-Rose system

The Hindmarsh-Rose (HR) system - one of the popular spike models has the form [49]:

$$\begin{cases} \dot{X} = Y + 3X^2 - X^3 - Z + I_{\text{ex}} \\ \dot{Y} = 1 - 5X^2 - Y \\ \dot{Z} = r \left[4(X + 8/5) - Z \right] \end{cases}, \quad (1)$$

where X is the membrane potential of the cell, Y and Z are the concentration of sodium and potassium ions, I_{ex} is the external current (stimulus), r is a small parameter characterizing the slow potassium current.

Figure 3a shows typical chaotic oscillograms of the variables of the HR model and the distances between the spikes for $X(t)$ (Figure 3b). Figure 4 shows a bifurcation diagram of the spike distances of the variable $X(t)$ with a change in the small parameter r for two values of the external current $I_{\text{ex}} = 3.25$ (Figure 4a) and $I_{\text{ex}} = 3.35$ (Figure 4b).

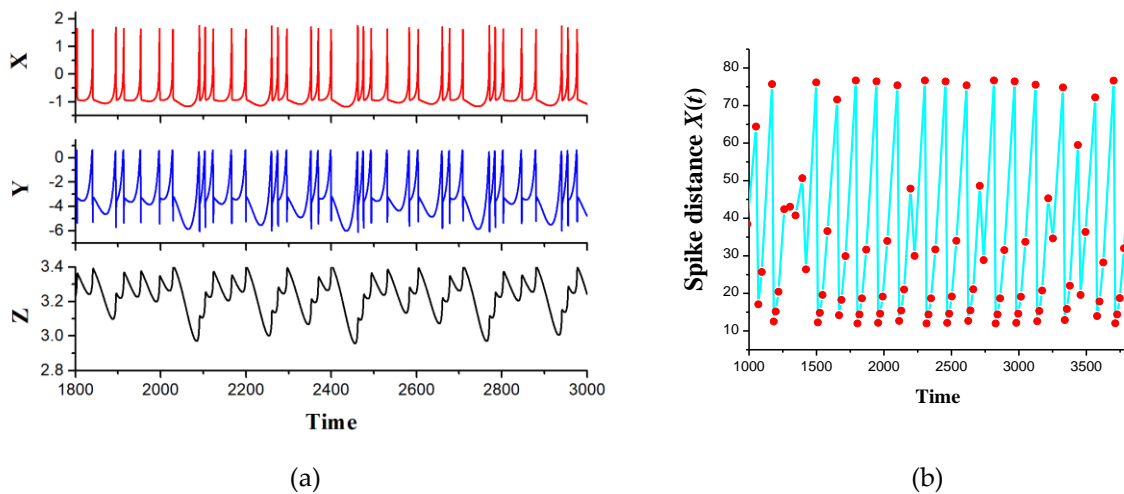


Figure 3. (a) Oscillograms of HR model variables calculated from equations (1). (b) Oscillogram of distances between spikes of cell membrane potential $X(t)$. Model parameter $r = 0.0055$.

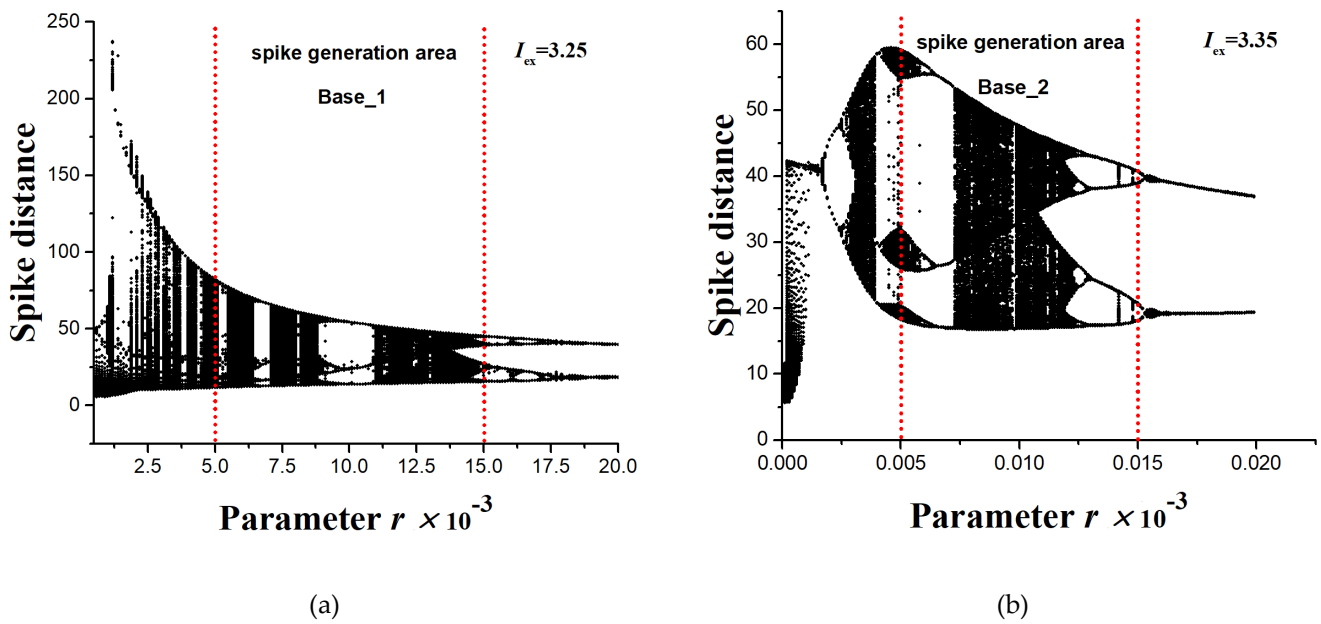


Figure 4. Bifurcation diagrams of distances between spikes of the HR model for the variable $X(t)$ with a change in the parameter r for two values of the external current (a) $I_{\text{ex}} = 3.25$ and (b) $I_{\text{ex}} = 3.35$. The region of spike generation for the Base_1 (a) and Base_2 (b) bases used for entropy calculation and perceptron training is shown. The diagrams also show the variety of chaotic and regular dynamics of oscillations with varying control parameters r and I_{ex} .

The dynamics of the HR model is well known [40,49] and is an alternation of regular and chaotic modes, which is very convenient for creating databases for training the perceptron as a chaos sensor.

2.3. Method for generating time series of various lengths

The method of generating time series of various lengths was used to generate databases and to study the dependence of the accuracy of the chaos sensor on the length of the time series. Sets of series of length NL from 10 to 100 elements, with a step of 10, were generated. Each set contained time series for both chaotic and regular regimes of spike oscillograms, which is controlled by the parameter r of equation (1). The variation range of r was $\{5 \cdot 10^{-3} \div 1.5 \cdot 10^{-2}\}$, as shown in Figure 4.

For a given value of r , an oscillogram was generated, which was then used to obtain a long time series with 500 elements. On the basis of one such long series, 100 short time series of the same length NL were generated. The principle of generation was to shift the window of a short time series along the main series with a step S (Figure 5). The step size was $S = 4$. This method made it possible to accumulate a dataset in which short series differed from each other, even if they belonged to the same state of the HR oscillator.

Thus, the series were generated in a wide variety and corresponded to the data flow to the chaos sensor in the continuous measurement mode.

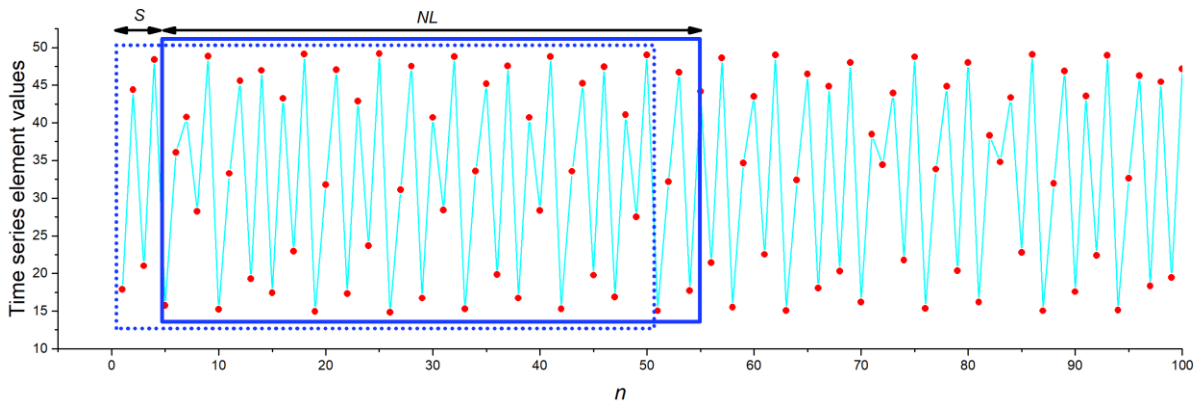


Figure 5. The principle of generating sets of short time series within one long time series. The blue frame indicates the short series window with a length of NL , which is shifted with step S .

2.4. Datasets for training and testing the perceptron

To train and test the perceptron, we used two different datasets Base_1 and Base_2, as well as their combination Base_1_2.

- The Base_1 dataset consisted of 10,000 time series with a length of $NL = 50$, which were obtained by modeling the HR system with $I_{ex} = 3.25$ (Figure 4a). The range of r was $\{5 \cdot 10^{-3} \div 1.5 \cdot 10^{-2}\}$ and divided into 100 values. The generation of 100 short time series for each r was performed according to the algorithm from Section 2.3. The target value of the entropy of all series was estimated through FuzzyEn according to the method from section 2.5.
- The Base_2 dataset consisted of 10,000 time series with a length of $NL = 50$, which were obtained by modeling the HR system with $I_{ex} = 3.35$ (Figure 4a). The range of r was $\{5 \cdot 10^{-3} \div 1.5 \cdot 10^{-2}\}$ and divided into 100 values. The generation of 100 short time series for each r was performed according to the algorithm from Section 2.3. The target value of the entropy of all series was estimated through FuzzyEn according to the method from section 2.5.
- Dataset Base_1_2 was a combination of Base_1 and Base_2.

The main characteristics of the datasets are presented in Table 1. The main characteristic is *Mean* - the average value for all elements of the time series. In addition, there are: *Mean50_min* - the minimum value of the average value of the time series, consisting of 50 elements; *Mean50_max* - the maximum value of the average value of the time series, consisting of 50 elements; *Min_X* - the minimum value of all elements in the dataset; *Max_X* - the maximum value of all elements in the dataset. Dataset files are available in the Supplementary Materials section.

Table 1. Characteristics of databases for training and testing the perceptron.

	<i>Mean</i>	<i>Mean50_min</i>	<i>Mean50_max</i>	<i>Min_X</i>	<i>Max_X</i>
Base_1	32.26571	30.09417	36.30281	11.686	81.764
Base_2	32.28749	29.70656	36.25960	16.744	59.124
Base_1_2	32.27660	29.70656	36.30281	11.686	81.764

Time series from databases were used to train and test the perceptron, one of the options was to pre-normalize the series.

Normalization was performed by subtracting from the values of the elements of the series the *Mean* value (Table 1).

2.5. Entropy calculation method

In the present study, we used FuzzyEn as the main method for assessing chaos, as it has good sensitivity when using short time series, a number of adjustable parameters, and a high calculation speed.

The principle of calculating FuzzyEn is based on measuring the conditional probability that if vectors (segments of a time series) of length m are similar, taking into account the allowable tolerance r_1 , then vectors of length $m + 1$ will be similar with the same allowable tolerance r_1 . The similarity metric between vectors is a fuzzy function calculated based on the distance between a pair of compared vectors.

The main variable parameters are: the length of the vector m , tolerance r_1 , and the type of the fuzzy function. In this work, an exponential fuzzy function of the form was chosen:

$$f(x) = \exp\left(\frac{x^{r_2}}{r_1}\right), \quad (2)$$

where r_2 is the power law exponent.

The range of variation during parameter optimization was for the m from 1 to 3, r_2 from 1 to 5, r_1 from $(0.005 - 0.4) \cdot \text{std}$, where std is the standard deviation of the elements of the time series.

To calculate the entropy, the python library EntropyHub was used.

It was found by the optimization method that the parameters FuzzyEn ($m = 1$, $r_2 = 1$, $r_1 = 0.01 * \text{std}$) provide the highest sensitivity for time series lengths from 10 to 100 elements.

2.6. Perceptron training and testing method

The goal of the study is to create the SPE model, which results, after training the perceptron, would match with the SFU model on R^2 metric in the best possible way.

To achieve this, it is necessary to train the perceptron to approximate FuzzyEn values. The datasets Base_1, Base_2, Base_1_2 and the scikit-learn python library were used to train and test the perceptron. Two-layer models were used with the number of neurons in the hidden layer 1, 50, and 150. The selection of model hyperparameters and accuracy assessment were carried out using the K-fold cross-validation method ($K = 10$). In this method, the dataset is divided into K-folds and the process of training and testing the model is carried out K times, each time one fold is used for testing, and all the rest make up the training set. As a metric for assessing the accuracy of the model, the coefficient of determination R^2 was used, which is calculated by the following equation:

$$R^2 = 1 - \frac{\sum_{i=1}^n (y_i - \hat{y}_i)^2}{\sum_{i=1}^n (y_i - \bar{y})^2}, \quad (3)$$

where y_i is the actual entropy value obtained in the SFU model, \hat{y}_i is the entropy value predicted by the SPE model, \bar{y} is the average actual entropy value of the SFU model.

To test the universality of the models, the method of training on one dataset and testing on another was also used.

3. Results

In this study, we present two models of the chaos sensor. The first model evaluates the irregularity of the time series through a FuzzyEn calculation called the SFU model (sensor). The second model estimates (approximates) the degree of chaos by a multilayer perceptron called the SPE model (sensor), this model is pre-trained on the results of the SFU model. The concept of the chaos sensor developed in the paper implies that a time series of a certain length NL is input, and the entropy value is calculated at the output. As an SPE sensor, we used a multilayer perceptron with the number of inputs equivalent to the length of the series NL . To answer the question of how the time series length affects the sensor characteristics, we generated sets of time series of various lengths NL from 10 to 100 elements, with a step of 10 according to the method from section 2.3. As the main characteristics of SFU and SPE sensors, the following were identified:

- $En_{av}(\text{chaos})$: average value of entropy over five chaotic series, at $r = 0.0056, 0.0076, 0.0082, 0.0119, 0.0141$ in HR model; Averaging within each series was carried out over 100 short series.
- $En_{av}(\text{order})$: average entropy value over five regular series, at $r = 0.0068, 0.0070, 0.0099, 0.0105, 0.0108$ in HR model; Averaging within each series was carried out over 100 short series.
- $EnR = En_{av}(\text{chaos}) - En_{av}(\text{order})$: range of entropy change at the output of the sensor.
- $Std_En(\text{chaos})$: entropy mean square deviation over five chaotic series;
- $Std_En(\text{order})$: entropy mean square deviation over five regular series;
- $EnSens = EnR / Std_En(\text{chaos})$: chaos sensor sensitivity.
- $EnErr = (Std_En(\text{chaos})/EnR) \cdot 100\%$: relative entropy measurement error in percent.

The presented characteristics were calculated at the current $I_{ex} = 3.25$.

The range of entropy change EnR is an important characteristic, as it shows how large the output range of the sensor is when the signal dynamics changes from order to chaos. The sensitivity of the $EnSens$ sensor shows how many times the mean square deviation is less than the range of entropy change. The relative measurement error ($EnErr$) shows the uncertainty of the output entropy value in percent, it is inversely proportional to the sensitivity. These characteristics may have different values in SFU and SPE sensor models.

Before calculating the dependence of sensor characteristics on NL , it is necessary to determine the optimal FuzzyEn entropy parameters, at which the sensitivity of the SFU model has maximum values for $NL = 10-100$. The optimization method found that the parameters FuzzyEn ($m = 1, r_2 = 1, r_1 = 0.01 \cdot std$) meet these requirements.

3.1. Dependence of sensor characteristics on the series length in the SFU model.

Figure 6a shows the dependences of $En_{av}(\text{chaos})$, $En_{av}(\text{order})$, and EnR on the length of the NL series for the SFU model. It can be seen that at $NL > 40$, the values of the characteristics saturate, which indicates the independence of the entropy values from the length of the series when this threshold is exceeded, and indicates the stability of the calculation of FuzzyEn on short time series with optimal parameters. As the series length decreases from $NL = 40$ to $NL = 10$, a significant increase in En_{av} (chaos) and EnR is observed. It is known that a decrease in the length of a series can lead to both an increase and a decrease in entropy, depending on the entropy parameters, as shown, for example, for NNetEn [36]. The value of the range of entropy change is of the order of $EnR \sim 3$, which is more than twice as large as En_{av} (order) and makes it possible to reliably record the chaotic behavior.

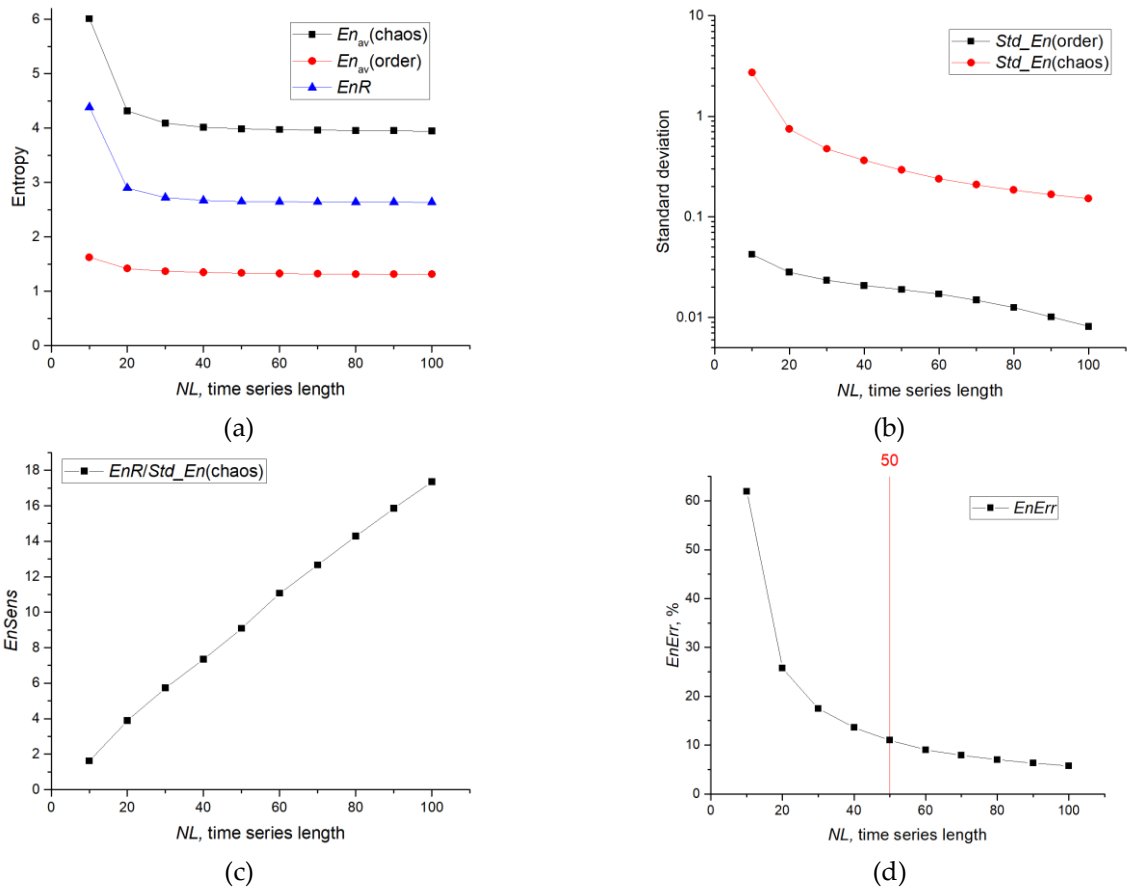


Figure 6. Dependence of chaos sensor characteristics on the length of the series in the SFU model (Sensor on FuzzyEn). The graphs show (a) $En_{av}(\text{chaos})$ and En_{av} (order), (b) $Std_En(\text{chaos})$ and $Std_En(\text{order})$, (c) $EnSens$ sensitivity, (d) $EnErr$ relative error.

Figure 6b shows the dependencies of $Std_En(\text{chaos})$ and $Std_En(\text{order})$ on NL . $Std_En(\text{chaos})$ exceeds $Std_En(\text{order})$ by more than an order of magnitude, and both characteristics decrease rapidly with increasing NL . At $NL = 50$, $Std_En(\text{chaos}) \sim 0.3$, which is approximately 10 times less than EnR . Figure 6c shows the dependence of the sensitivity of the $EnSens$ sensor on the length NL series. It can be seen that $EnSens$ increases linearly with the length of the time series, which indicates a better measurement of chaos on long series. The increase in $EnSens$ is mainly associated with a decrease in the standard deviation $Std_En(\text{chaos})$, since EnR practically does not change from NL . The relative entropy measurement error $EnErr$ as a function of NL is shown in Figure 6d. The maximum measurement error $EnErr \sim 60\%$ is observed at the minimum time series length $NL = 10$ and quickly decreases to $EnErr \sim 11\%$ at $NL = 50$. In our opinion, the measurement $EnErr$ error $\leq 11\%$ can be considered acceptable in practice, and time series are needed for the sensor with length $NL \geq 50$.

3.2. Results of entropy approximation in perceptron SPE model

To train the perceptron, the series length $NL = 50$ was chosen based on the results of the previous section, where it is shown that for the SFU model, the error is $EnErr \sim 11\%$.

Table 2 presents the results of estimation of the coefficient of determination R^2 for perceptron models with the number of neurons in the hidden layer $NH = 1, 50$ and 150 . Preliminary normalization was not carried out. Various combinations of training and test databases were evaluated in the condition of submitting time series without normalization. It can be seen that for $NH = 1$, the models poorly approximated the entropy in all cases. At $NH = 50$ and $NH = 150$, the approximation had high values of $R^2 \sim 0.8-0.88$ when using the cross-validation method within the baseline. At the same time, the model with

a large number of neurons in the hidden layer $NH = 150$ showed the best results. It can be seen that cross-validation within the combined base Base_1_2 showed high results, although separately training on one base and testing on another low R^2 values. This indicates that the model is being over trained on a separate base and is not suitable for working with another base. In general, the approach without normalization can be applied in practice if the training base contains all possible combinations of time series, as in the case of Base_1_2.

Table 2. Approximation accuracy estimation by the R^2 metric without the normalization stage

Number of neurons in the hidden layer, NH	Cross-validation accuracy, R^2			Approximation accuracy when training on one base and testing on another, R^2	
	Base_1	Base_2	Base_1_2	Base_1-Training	Base_1-Testing
	Base_2-Testing	Base_2-Training			
1	-0.001	-0.001	-0.001	-0.013	-0.047
50	0.827	0.868	0.810	0.030	-0.084
150	0.846	0.888	0.842	0.159	-0.831

Table 3 presents the results of estimation of the coefficient of determination R^2 for perceptron models with the number of neurons in the hidden layer $NH = 1, 50$ and 150 , in the condition of preliminary normalization of time series. Normalization was performed by subtracting from the values of the elements of the series the value of the average value *Mean* (Table 1).

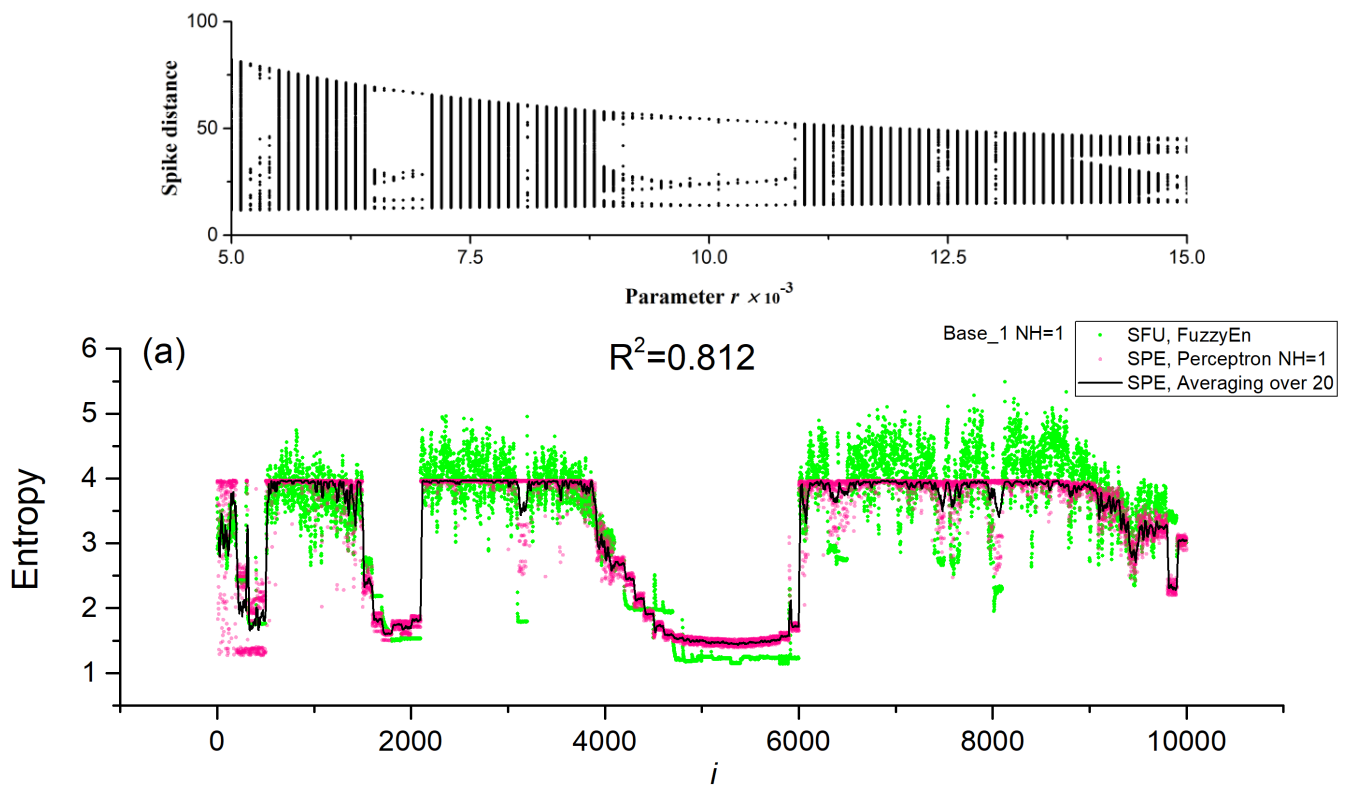
Table 3. Approximation accuracy estimation by metric R^2 using the normalization stage.

Number of neurons in the hidden layer, NH	Cross-validation accuracy, R^2			Approximation accuracy when training on one base and testing on another, R^2	
	Base_1	Base_2	Base_1_2	Base_1-Training	Base_1-Testing
	Base_2-Testing	Base_2-Training			
1	0.812	0.617	0.498	0.128	0.326
50	0.904	0.928	0.885	-0.180	0.655
150	0.912	0.937	0.897	-0.729	0.568

Models with one neuron in the hidden layer ($NH = 1$) had high values of $R^2 \sim 0.5-0.8$ in the cross-validation mode. The largest $R^2 \sim 0.8$ corresponded to Base_1, the smallest $R^2 \sim 0.5$ to the combined Base_1_2. These results allow us to state that even a single neuron in the hidden layer approximates entropy well, although the accuracy of the model decreases with an increase in the variety of time series when the bases are combined (Base_1_2). Figure 7a shows the dependence of FuzzyEn for the SFU model on the series number in Base_1 and the dependence predicted by the SPE model with one neuron (Perceptron $NH = 1$). In addition, the graph shows the average value over 20 measurements for the SPE model (Averaging over 20). It can be seen that the perceptron model predicts well the FuzzyEn entropy values, repeating the regions with high and low entropy values. To confirm the correctness of the calculation of the SFU and SPE models, the insertion of the bifurcation diagram of the HR model corresponding to the Base_1 numbering is given. It can be seen that the areas of chaos and order correspond to each other. The average value repeats the entropy dependence even better, having less fluctuation. A more detailed study of the physics of the perceptron model with one neuron is discussed in the

next section. An increase in the number of neurons in the hidden layer enhances the accuracy of the perceptron SPE model, reaching $R^2 \sim 0.9$ for all bases in the cross-validation mode. In general, the difference between $NH = 50$ and $NH = 150$ is not very significant, and it is acceptable to use $NH = 50$ in practice. Figure 7b shows the entropy curve for the SPE model with $NH = 50$ and Base_1. The perceptron model in this case reproduces the nuances of FuzzyEn very well, and the average value (Averaging over 20) correctly tracks even very narrow regions of order and chaos.

The model with normalization performed very well when testing and training on different bases. So, with $NH = 50$, training on Base_2, and testing on Base_1 showed $R^2 \sim 0.655$, when the bases are changed in places, the approximation deteriorates to $R^2 \sim -0.18$. This suggests that it is better to use Base_2 for training, since it contains more variants present in Base_1, and is more versatile. When combining Base_1_2 bases, cross-validation shows improved values of $R^2 \sim 0.885$. Figure 7c shows the dependences of the entropies for $NH = 50$ and Base_1 in the case of training the model on Base_2. It can be seen that the model track segments with regular time series worse, but in general it guesses FuzzyEn values with acceptable accuracy.



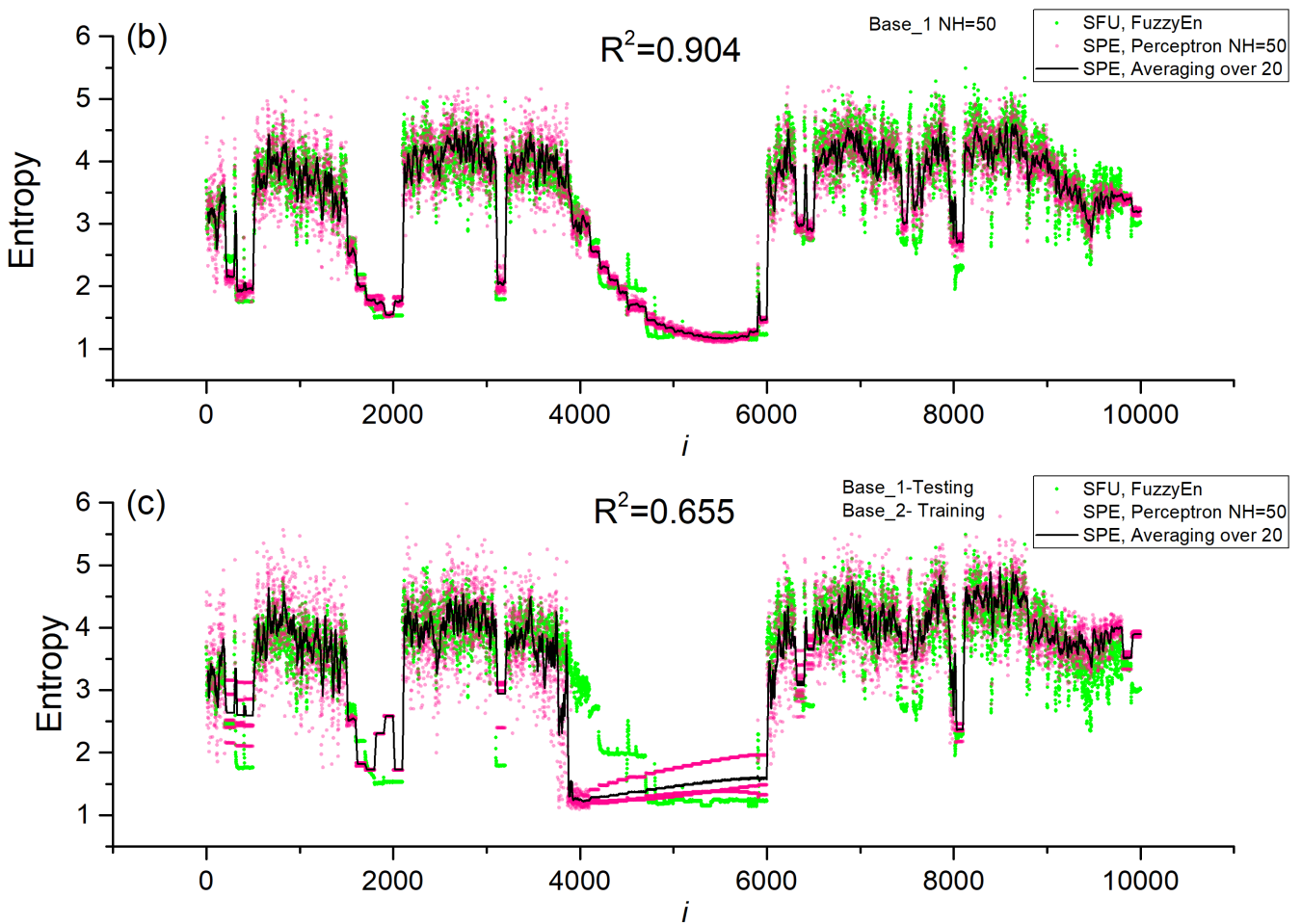


Figure 7. Dependences of entropy on the element number in Base_1 for SFU and SPE models, as well as the average value over 20 measurements for SPE (Averaging over 20). Results are shown for models (a) Base_1 and $NH = 1$, (b) Base_1 and $NH = 50$, (c) Base_1 – testing, Base_2 - training. The inset to figure (a) shows the bifurcation diagram of the HR model corresponding to Base_1.

Figure 8a shows the dependences of the entropies of SFU and SPE sensors for $NH = 50$ and Base_2 after cross-validation. The perceptron model perfectly approximates FuzzyEn with an accuracy of $R^2 \sim 0.928$. To confirm the correctness of the calculation of SFU and SPE models, the bifurcation diagram of the HR model corresponding to the Base_2 numbering is inserted. It can be seen that the areas of chaos and order correspond to each other. Figure 8b shows the dependences of the entropies of SFU and SPE sensors for $NH = 50$ and Base_2 in the case of training the model on Base_1. It can be seen that the SPE model poorly tracks segments with regular time series for $i < 2500$, but it is good at guessing chaotic segments and part of regular ones for $i > 2500$. This leads to the fact that the estimate of the approximation accuracy decreases to $R^2 \sim 0.18$. It can be concluded that it is better to use Base_2 for training, since it contains more options present in Base_1, and is more versatile.

Figure 9 shows the entropy dependences for $NH = 50$ for the combined base Base_1_2 after cross-validation. The perceptron model approximates well the FuzzyEn values for both bases with an accuracy of $R^2 \sim 0.885$. The good accuracy of the approximation allows this model to be used in practice. Table 4 shows the main characteristics of the chaos sensor at $NL = 50$ for the SFU model, perceptron SPE model ($R^2 \sim 0.928$) and averaging (SPE Averaging over 20). The perceptron model is not inferior to the SFU model in terms of the $EnSens$ and $EnErr$ parameters, while averaging gives a significant increase in sensitivity and a decrease in the relative measurement error by almost 3 times to 4%.

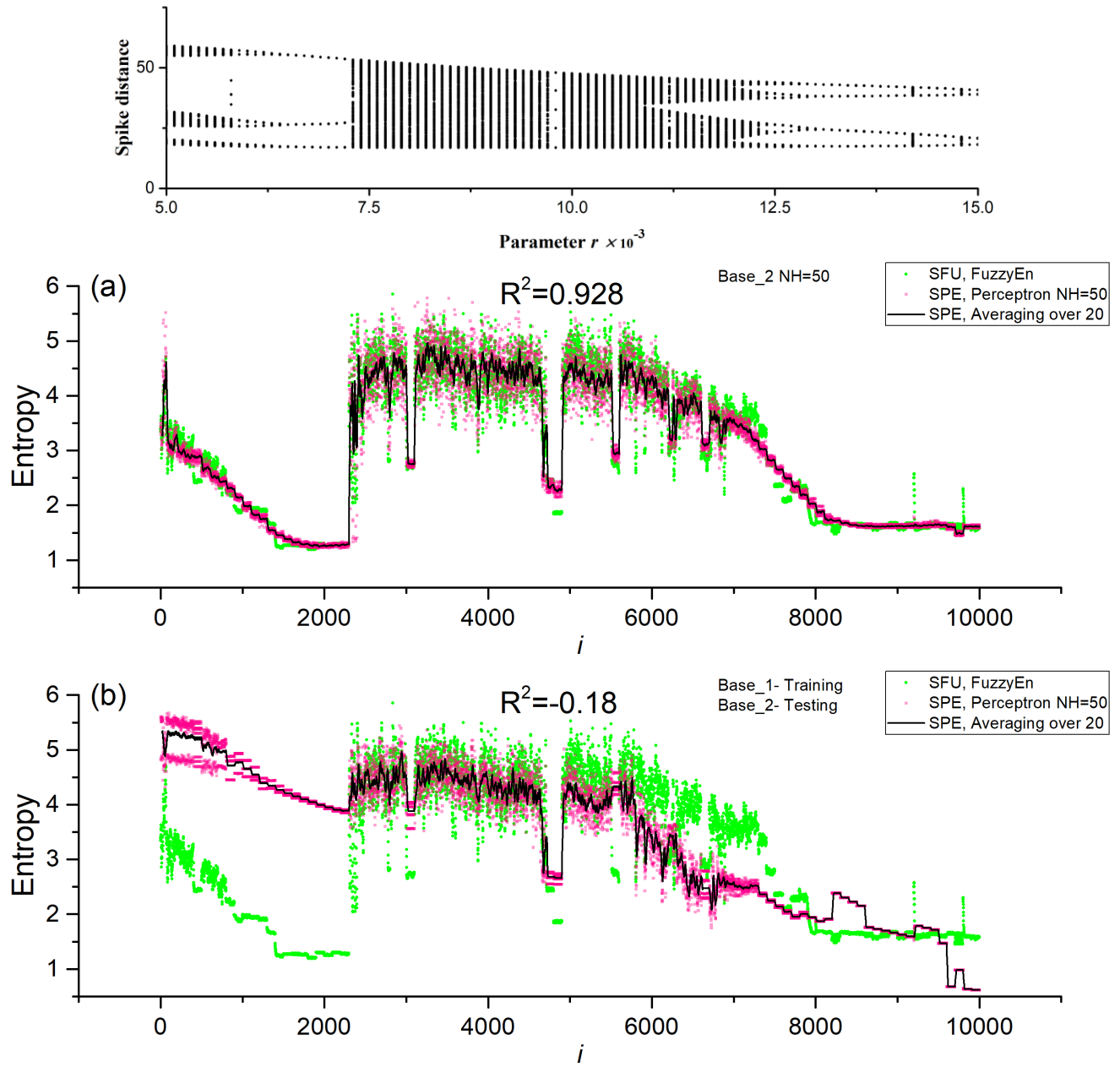


Figure 8. Dependences of entropy on the element number in Base_2 for SFU and SPE models, as well as the average value over 20 measurements for SPE (Averaging over 20). Results are shown for models $NH = 50$, (a) Base_2, (b) Base_2 – testing, Base_1 - training. The inset to figure (a) shows the bifurcation diagram of the HR model corresponding to Base_2.

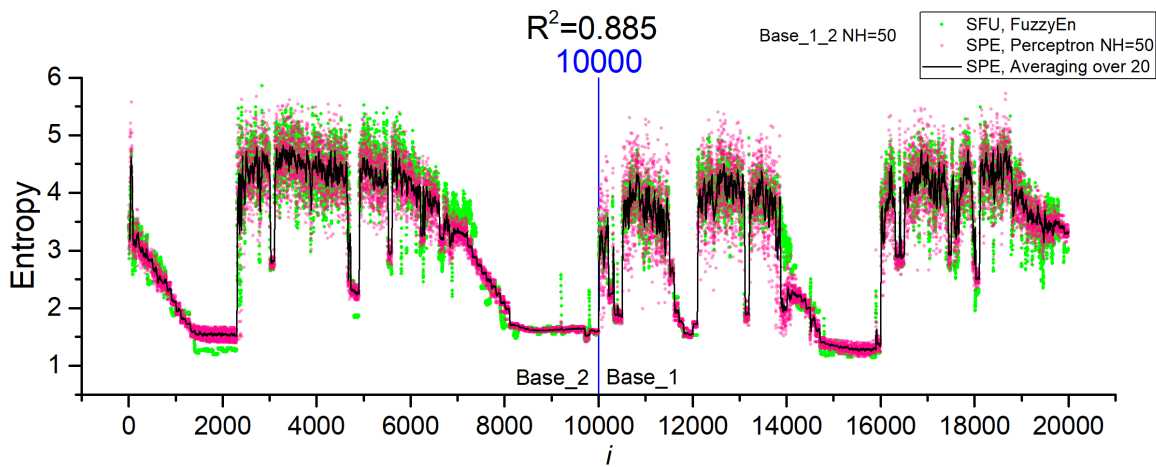


Figure 9. Dependences of entropy on the element number in Base_1_2 for SFU and SPE models, as well as the average value over 20 measurements for SPE (Averaging over 20). The results are shown for the $NH = 50$ model for the combined base Base_1_2.

Table 4. Chaos sensor characteristics at $NL = 50$ for SFU model, perceptron SPE model ($R^2 \sim 0.928$) and averaging (SPE Averaging over 20). Perceptron model $NH = 50$ for Base_2 after cross-validation.

	$En_{av}(\text{order})$	$En_{av}(\text{chaos})$	$Std_En(\text{chaos})$	$EnSens$	$EnErr$
Sensor on FuzzyEn	1.33	3.98	0.29	9	11%
Sensor on Perceptron	1.48	4	0.28	9	11%
Sensor on Perceptron	1.34	4.1	0.11	25	4%
Averaging over 20					

3.3. Operating principles of the perceptron sensor model

The results of the previous section showed that the use of normalization significantly improves the performance of the SPE chaos sensor. It was also found that the sensor can work with acceptable accuracy even with one neuron in the hidden layer. There is a natural desire to understand the principle of the sensor. To do this, consider the distribution of weights in the perceptron with one neuron in the hidden layer (Figure 11). The figure shows three options for the distribution of weights for a model based on Base_1 (Figure 11a), Base_2 (Figure 11b) and Base_1_2 (Figure 11c). All three distributions have a common pattern, expressed in the fact that all weights are positive and have values near the average, indicated by a solid horizontal line in each figure. This regularity suggests the assumption to replace all weights with the same values equivalent to the average value. As a result, for Base_1 we get the perceptron model shown in Figure 10d. The figure shows the values of all weights. Such a simplified perceptron gives the approximation accuracy $R^2 \sim 0.747$ for Base_1, $R^2 \sim 0.236$ for Base_2, $R^2 \sim 0.447$ for Base_1_2. The dependencies of entropy on the element number in Base_1 for the SFU and SPE models are shown in Figure 11. It can be seen that the SPE model roughly approximates the SFU model, however, it traces the main areas of order and chaos reasonably. Such a simple model actually does the averaging of the time series, and the value of the average is then linearly transformed into entropy

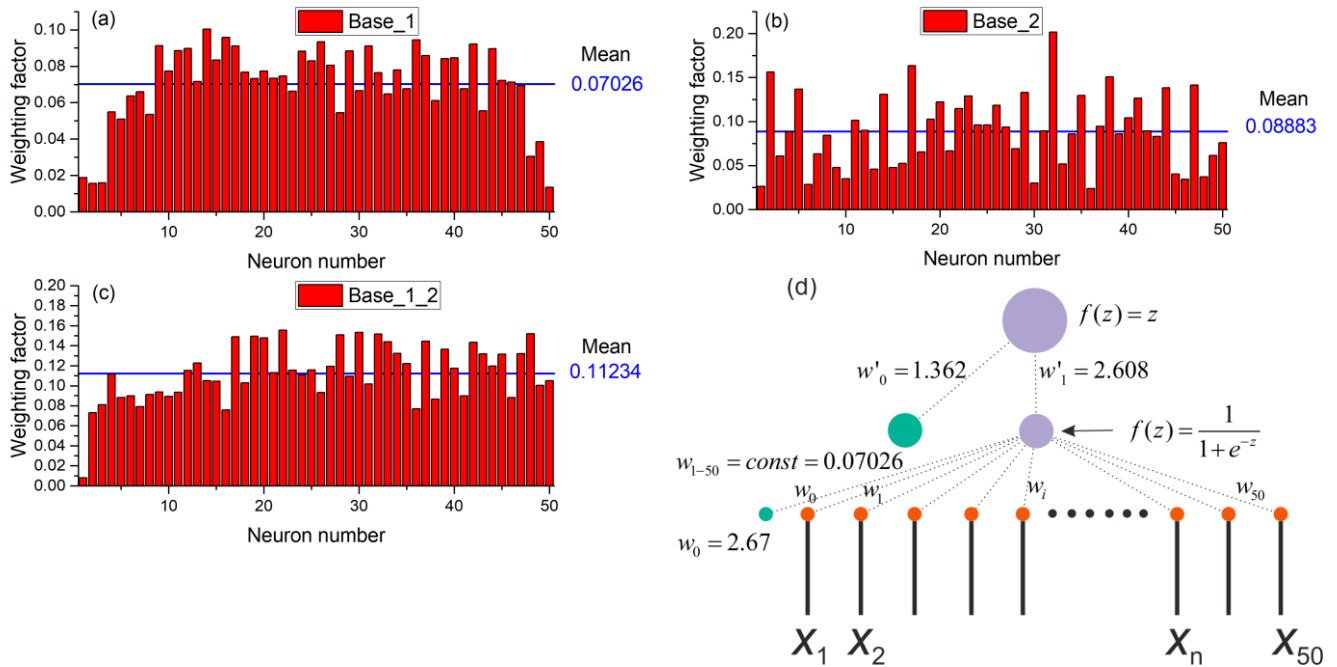


Figure 10. Distributions of weights for the perceptron model based on one neuron in the hidden layer for (a) Base_1, (b) Base_2 and (c) Base_1_2. (c) Perceptron model with equal weights from input to hidden neuron. The figure shows all the weights of the simplified model of the chaos sensor.

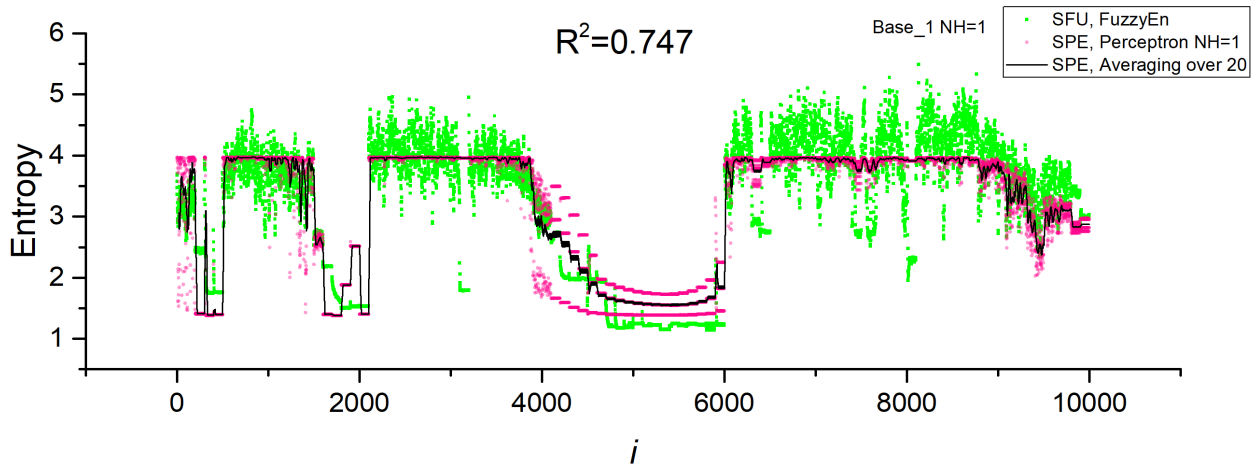


Figure 11. Dependences of entropy on the element number in Base_1 for SFU and SPE models, as well as the average value over 20 measurements for SPE (Averaging over 20). The results are shown for a simplified model with one $NH = 1$ neuron and equal weights. Calculations were made on Base_1.

The SPE model with one neuron and weights fitted during training is a much better approximation (Figure 7a) than the simplified model (Figure 11). The SPE model with a large number of neurons in the hidden layer approximates the entropy even better for various combinations of bases (Table 3). Figure 12 shows a perceptron model with 50 neurons in the hidden layer. The weights from the hidden layer to the output neuron are presented as a histogram in Figure 12a, the distribution of weights from the input layer to the hidden layer is shown in Figure 12b. The general model of the perceptron is shown in Figure 12c. The principle of functioning of the sensor on the distribution of weights is difficult to explain and additional research is needed in this direction. Nevertheless, it can be assumed that the input time series is convolved with certain weight patterns, which

are also time series, possibly the most frequently occurring in the database, and then the result of the convolution is written to the neurons of the hidden layer. The weights have both positive and negative values, which is similar to the time series after the normalization step. The hidden layer neuron value vector is then convolved with the output layer weights, which also have positive and negative values. In the case of a regular time series input, the result of the convolution has a reduced value, in the case of a chaotic series it has an increased value.

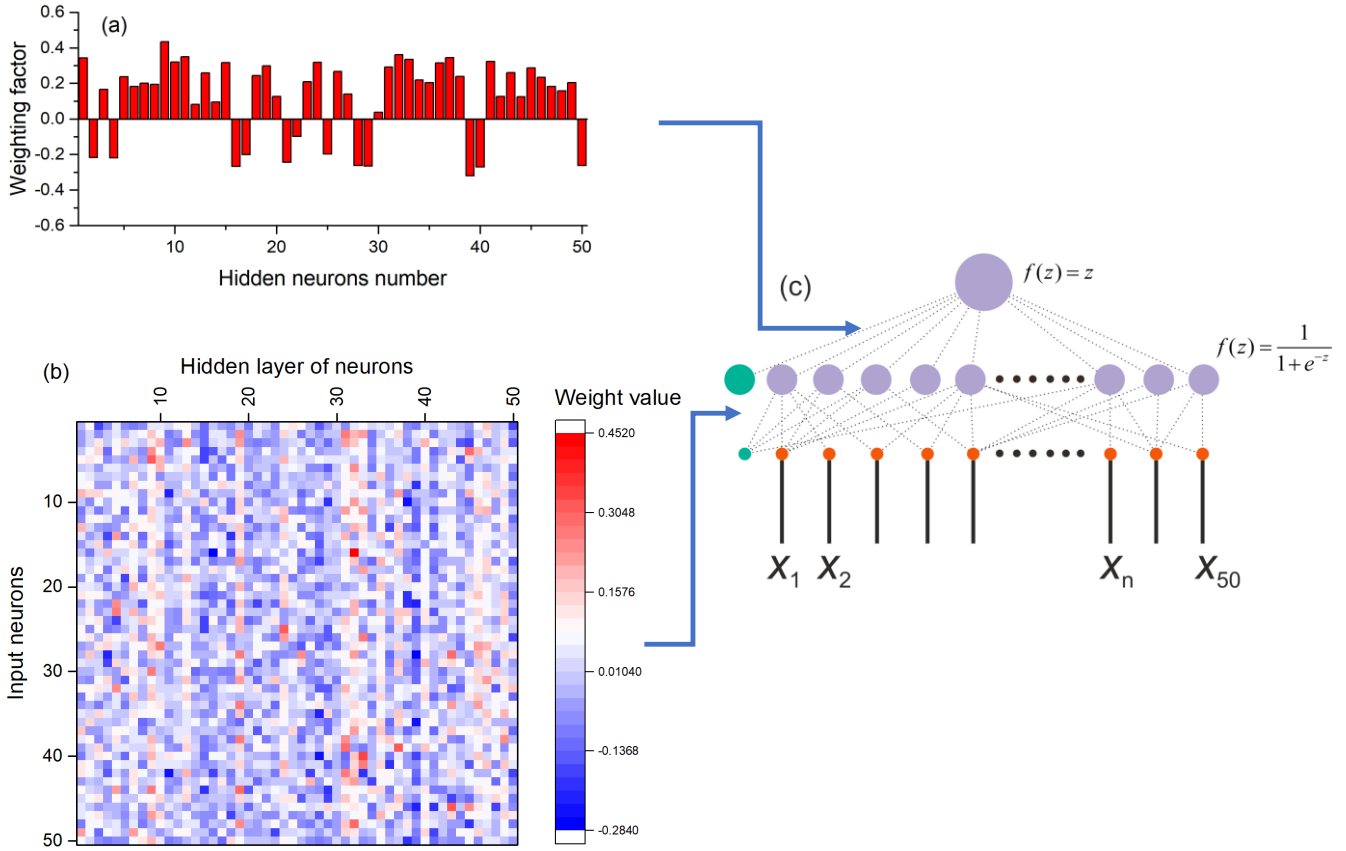


Figure 12. Perceptron model with 50 neurons in the hidden layer. The weights from the hidden layer to the output neuron are presented as a histogram (a), the distribution of weights from the input layer to the hidden layer is shown in figure (b). The general model of the perceptron is shown in Figure (c).

4. Discussion

In biology and medicine, as in other fields of science, there are systems that combine the properties of regular and irregular dynamics and exhibit the properties of deterministic chaos that arises and disappears when the parameters vary. Chaos appears in a variety of studies of wildlife from biochemistry and genetics to population biology and ecology, in which it can serve as an indicator of instability, development, imminent death, "right" and "wrong" processes (see Introduction). A question may arise: *Can the biosystem itself evaluate the randomness of signals?* In the course of this study, we found out that it is quite realistic to create a bio-inspired model of a chaos sensor based on a multi-layer perceptron. One of the popular spike models used to describe real biological neurons, the Hindmarsh-Rose system, was considered. It allows modeling spike activity in a wide range of spike dynamics, with the presence of chaotic and regular modes with many patterns controlled by the system parameters r and I_{ex} . Examples of spike waveforms and bifurcation diagrams have been demonstrated in Figures 3-4. It is worth mentioning here

that we tested the perceptron-based sensor precisely within the Hindmarsh-Rose model, we do not claim that the model can be applied directly, with the same coefficients, to other models of spike activity or synthetic time series, in each case requires additional research. Nevertheless, it is clear that in a particular biological system, most likely, the spike activity also changes within a certain model system, and it is always possible to train the perceptron to distinguish between chaos and order in this particular biosystem (living organism). The question of the actual presence of an ensemble of neurons with a similar function as a chaos sensor may be the subject of future research by neurophysiologists. The paper proposes a bio-inspired tool for assessing chaos, but the question whether it is used or not in nature remains open. The authors suggest that as a result of evolution, complex combinations of neurons could have arisen that work as a sensor of chaos. Moreover, in an elementary model with one neuron and the same weights (Figure 10), the sensor is the simplest integrator, which can also be implemented on other elements, for example, on an integrating RC circuit. The development of these ideas may be a topic for further research.

The idea of a chaos sensor is based on training the perceptron to determine the value of the entropy of the time series entering its input. The time series is a set of distances between spikes, with a length of 10 to 100 elements. This approach is model, since it is obvious that nature operates with spikes, and not with distances between them, and in a real biosystem, a time series is not allocated and is not fed to the perceptron as in a computer. Nevertheless, the perceptron model is used very widely in neuroscience, and it can qualitatively describe complex processes. In the future, it is possible to work with real spike systems, for example, of a reservoir type and model the entropy approximation, such studies will be a promising direction for the development of this work.

In this paper, we presented the SFU and SPE models of the chaos sensor. The first model estimates the irregularity of the time series through the calculation of FuzzyEn, the second model approximates the degree of chaos with a multilayer perceptron. The main goal was to create an SPE model, that match the SFU model as best as possible in terms of the R^2 metric, after training the perceptron. At the beginning of the 3rd section, the main parameters of the chaos sensor are introduced, such as the sensitivity $EnSens$ and the measurement error $EnErr$. FuzzyEn was chosen as a measure of entropy. The selection of its parameters made it possible to achieve a high sensitivity of the sensor on short time series (Figure 6) and a low measurement error. Thus, for the length of the series $NL = 50$, the entropy measurement error by the perceptron was at the level of $EnErr \sim 11\%$ (Table 4, Sensor on Perceptron). The error can be reduced by averaging the result, for example, averaging over 20 results reduces the measurement error to $EnErr \sim 4\%$, almost 3 times (Table 4). It is clear that averaging over the result is equivalent to increasing the length of the time series. And as can be seen from Figure 6 c,d, an increase in the length of the series leads to an increase in $EnSens$ and a decrease in EnR . Nevertheless, from a practical point of view, it is more difficult to work with long series, including the perceptron, and averaging can be easily implemented both in model and real biosystems. Thus, averaging makes it possible to work with even shorter series $NL = 10, 20$. The study of the characteristics of the chaos sensor and the approximation of the perceptron to ultrashort series can be the subject of further research.

As the results of tables 2 and 3 showed, the correct normalization of the time series can significantly increase the accuracy of the approximation of the perceptron models. In general, the approach without normalization can be applied in practice if the training base contains all possible combinations of time series, as in the case of Base_1_2. The technique of training on one base and testing on another showed low R^2 values (Table 2, last 2 columns). On the one hand, this indicates that the model is over trained on a separate base and is not suitable for working with another base. It shows that the two bases Base_1 and Base_2 have a different set of time series, which is also noticeable in the buffer diagrams (Figure 4) and Table 1, where the Min_X and Max_X of the two bases differ significantly. Such a difference was created by us intentionally in order to test the universality of the created perceptron models as a chaos sensor.

The normalization method was to subtract from the values of the elements of the series the value of the average value *Mean* (Table 1). The results are presented in Table 3 and are significantly better than without normalization. The results suggest that even a single neuron in the hidden layer approximates the entropy well, although the accuracy of the model decreases with an increase in the variety of time series when bases are combined. This is also noticeable when training on one base and testing on another (Table 3, last 2 columns). However, R^2 reaches values of $R^2 \sim 0.326$ when training on Base_2 and testing on Base_1, which indicates a partial approximation. The reason for the unsatisfactory approximation, in our opinion, lies in the fact that the principle of operation of a perceptron with one neuron in the hidden layer is related to the average value of the time series (Section 3.3), however, many variants of the time series do not obey this pattern.

The model with normalization and a large number of neurons in the hidden layer $NH = 50, 150$ approximates the FuzzyEn values with an acceptable accuracy of $R^2 \sim 0.9$ (Figure 7b, 8a). The principle of functioning of the sensor according to the distribution of weights (Figure 12) is difficult to explain and additional research is needed in this direction. However, it can be assumed that the input time series is rolled up with certain weight patterns representing the most frequently occurring time series in the database. Then the resulting vector of hidden layer neuron values is convolved with the weights of the output layer, which also have positive and negative values. In the case of a regular time series input, the result of the final convolution has a lower value; in the case of a chaotic series, it has an increased value.

5. Conclusions

As a result of the study, a biosimilar model of a chaos sensor based on a multilayer perceptron was proposed and investigated. We tested the perceptron-based sensor within the Hindmarsh-Rose model, we do not claim that the perceptron model can be applied directly, with the same coefficients, to other models of spike activity or synthetic time series, in each case additional studies are required. Thus, we have given a positive answer to the question: *Can the biosystem itself evaluate the randomness of signals?*

A perceptron model with 1 neuron in the hidden layer is proposed, which allows obtaining a high degree of similarity between SFU and SPE models for short series of length $NL = 50$. A perceptron model with 50 neurons in the hidden layer is proposed, which allows obtaining a very high degree of similarity between SFU and SPE models with an accuracy of $R^2 \sim 0.9$. Potentially, a chaos sensor for short time series makes it possible to dynamically track the chaotic behavior of neuron impulses and transmit this information to other parts of the biosystem. We hope that the work will be useful for specialists in the field of computational neuroscience, and our team is ready to interact with interested parties in joint projects.

Supplementary Materials: The following supporting information can be downloaded at: www.mdpi.com/xxx/ datasets.zip Database Base_1, Base_2 and Base_1_2.

Author Contributions: Conceptualization, A.V.; methodology, A.V., P.B., M.B. and V.P.; software, A.V., P.B., M.B. and V.P.; validation, M.B. and V.P.; formal analysis, A.V.; investigation, A.V., M.B. and V.P.; resources, P.B.; data curation, A.V.; writing—original draft preparation, A.V., P.B., M.B. and V.P.; writing—review and editing, A.V., P.B., M.B. and V.P.; visualization, A.V., P.B., M.B. and V.P.; supervision, A.V.; project administration, A.V.; funding acquisition, A.V. All authors have read and agreed to the published version of the manuscript.

Funding: This research was supported by the Russian Science Foundation (grant no. 22-11-00055, <https://rscf.ru/en/project/22-11-00055/>, accessed on 30 March 2023).

Institutional Review Board Statement: Not applicable.

Data Availability Statement: The data used in this study can be shared with the parties, provided that the article is cited.

Acknowledgments: The authors express their gratitude to Andrei Rikkiev for valuable comments made in the course of the article's translation and revision. Special thanks to the editors of the journal and to the anonymous reviewers for their constructive criticism and improvement suggestions.

Conflicts of Interest: The authors declare no conflict of interest.

References

1. Hänggi, P. Stochastic Resonance in Biology How Noise Can Enhance Detection of Weak Signals and Help Improve Biological Information Processing. *Chemphyschem* **2002**, *3*, 285–290, doi:10.1002/1439-7641(20020315)3:3<285::AID-CPHC285>3.0.CO;2-A.
2. McDonnell, M.; Ward, L. The Benefits of Noise in Neural Systems: Bridging Theory and Experiment. *Nat. Rev. Neurosci.* **2011**, *12*, 415–425, doi:10.1038/nrn3061.
3. Takahashi, T. Complexity of Spontaneous Brain Activity in Mental Disorders. *Prog. Neuro-Psychopharmacology Biol. Psychiatry* **2013**, *45*, 258–266, doi:<https://doi.org/10.1016/j.pnpbp.2012.05.001>.
4. Vd Groen, O.; Tang, M.; Wenderoth, N.; Mattingley, J. Stochastic Resonance Enhances the Rate of Evidence Accumulation during Combined Brain Stimulation and Perceptual Decision-Making. *PLOS Comput. Biol.* **2018**, *14*, e1006301, doi:10.1371/journal.pcbi.1006301.
5. Freeman, W.J. Simulation of Chaotic EEG Patterns with a Dynamic Model of the Olfactory System. *Biol. Cybern.* **1987**, *56*, 139–150, doi:10.1007/BF00317988.
6. Moss, F.; Ward, L.M.; Sannita, W.G. Stochastic Resonance and Sensory Information Processing: A Tutorial and Review of Application. *Clin. Neurophysiol.* **2004**, *115*, 267–281, doi:<https://doi.org/10.1016/j.clinph.2003.09.014>.
7. Garrett, D.; Samanez-Larkin, G.; MacDonald, S.; Lindenberger, U.; McIntosh, A.; Grady, C. Moment-to-Moment Brain Signal Variability: A next Frontier in Human Brain Mapping? *Neurosci. Biobehav. Rev.* **2013**, *37*, 610–624, doi:10.1016/j.neubiorev.2013.02.015.
8. Hindmarsh, J.; Rose, R. A Model of Neuronal Bursting Using Three Coupled First Order Differential Equations. *Proc. R. Soc. Lond. B. Biol. Sci.* **1984**, *221*, 87–102, doi:10.1098/rspb.1984.0024.
9. S.A., M.; A.H., M. Synchronization of Hindmarsh Rose Neurons. *Neural Networks* **2020**, *123*, 372–380, doi:<https://doi.org/10.1016/j.neunet.2019.11.024>.
10. Shilnikov, A.; Kolomiets, M. Methods of the Qualitative Theory for the Hindmarsh-Rose Model: A Case Study - a Tutorial. *I. J. Bifurc. Chaos* **2008**, *18*, 2141–2168, doi:10.1142/S0218127408021634.
11. Kumar, A. CHAOS THEORY: IMPACT ON AND APPLICATIONS IN MEDICINE. *J. Heal. Allied Sci. NU* **2012**, *02*, 93–99, doi:10.1055/s-0040-1703623.
12. Pappalettera, C.; Miraglia, F.; Cotelli, M.; Rossini, P.M.; Vecchio, F. Analysis of Complexity in the EEG Activity of Parkinson's Disease Patients by Means of Approximate Entropy. *GeroScience* **2022**, *44*, 1599–1607, doi:10.1007/s11357-022-00552-0.
13. Morabito, F.C.; Labate, D.; La Foresta, F.; Bramanti, A.; Morabito, G.; Palamara, I. Multivariate Multi-Scale Permutation Entropy for Complexity Analysis of Alzheimer's Disease EEG. *Entropy* **2012**, *14*, 1186–1202, doi:10.3390/e14071186.
14. Acharya, U.R.; Fujita, H.; Sudarshan, V.K.; Bhat, S.; Koh, J.E.W. Application of Entropies for Automated Diagnosis of Epilepsy Using EEG Signals: A Review. *Knowledge-Based Syst.* **2015**, *88*, 85–96, doi:10.1016/j.knosys.2015.08.004.
15. Xu, X.; Nie, X.; Zhang, J.; Xu, T. Multi-Level Attention Recognition of EEG Based on Feature Selection. *Int. J. Environ. Res. Public Health* **2023**, *20*, 3487, doi:10.3390/ijerph20043487.
16. Stancin, I.; Cifrek, M.; Jovic, A. A Review of EEG Signal Features and Their Application in Driver Drowsiness

Detection Systems. *Sensors* **2021**, *21*, 3786, doi:10.3390/s21113786.

17. Richer, R.; Zhao, N.; Amores, J.; Eskofier, B.M.; Paradiso, J.A. Real-Time Mental State Recognition Using a Wearable EEG. In Proceedings of the 2018 40th Annual International Conference of the IEEE Engineering in Medicine and Biology Society (EMBC); IEEE, July 2018; pp. 5495–5498.

18. Duan, R.-N.; Zhu, J.-Y.; Lu, B.-L. Differential Entropy Feature for EEG-Based Emotion Classification. In Proceedings of the 2013 6th International IEEE/EMBS Conference on Neural Engineering (NER); IEEE, November 2013; pp. 81–84.

19. Lu, Y.; Wang, M.; Wu, W.; Han, Y.; Zhang, Q.; Chen, S. Dynamic Entropy-Based Pattern Learning to Identify Emotions from EEG Signals across Individuals. *Measurement* **2020**, *150*, 107003, doi:10.1016/j.measurement.2019.107003.

20. Mu, Z.; Hu, J.; Min, J. EEG-Based Person Authentication Using a Fuzzy Entropy-Related Approach with Two Electrodes. *Entropy* **2016**, *18*, 432, doi:10.3390/e18120432.

21. Thomas, K.P.; Vinod, A.P. Biometric Identification of Persons Using Sample Entropy Features of EEG during Rest State. In Proceedings of the 2016 IEEE International Conference on Systems, Man, and Cybernetics (SMC); IEEE, October 2016; pp. 003487–003492.

22. Churchland, P.S. *The Computational Brain / Patricia S. Churchland and Terrence J. Sejnowski*; Sejnowski, T.J. (Terrence J., Ed.); Computational neuroscience.; MIT Press: Cambridge, Mass, 1992; ISBN 0262031884.

23. Maass, W.; Legenstein, R.; Markram, H.; Bülthoff, H.; Lee, S.-W.; Poggio, T.; Wallraven, C. *A New Approach towards Vision Suggested by Biologically Realistic Neural Microcircuit Models*; 2002; Vol. 2525; ISBN 978-3-540-00174-4.

24. Bahmer, A.; Gupta, D.; Effenberger, F. Modern Artificial Neural Networks: Is Evolution Cleverer? *Neural Comput.* **2023**, *35*, 763–806, doi:10.1162/neco_a_01575.

25. Rumelhart, D.E.; McClelland, J.L.; Group, P.D.P.R. Parallel Distributed Processing: Explorations in the Microstructure of Cognition: Foundations 1986.

26. Plaut, D.C.; McClelland, J.L.; Seidenberg, M.S.; Patterson, K. Understanding Normal and Impaired Word Reading: Computational Principles in Quasi-Regular Domains. *Psychol. Rev.* **1996**, *103*, 56–115, doi:10.1037/0033-295x.103.1.56.

27. Elman, J.; Bates, E.; Johnson, M.; Karmiloff-Smith, A.; Parisi, D.; Plunkett, K. *Rethinking Innateness: A Connectionist Perspective On Development*; 1996; ISBN 9780262272292.

28. Marcus, G. *The Algebraic Mind: Integrating Connectionism and Cognitive Science*; 2001; ISBN 9780262279086.

29. Rosenblatt, F. The Perceptron: A Probabilistic Model for Information Storage and Organization in the Brain [J]. *Psychol. Rev.* **1958**, *65*, 386–408, doi:10.1037/h0042519.

30. Rumelhart, D.; Hinton, G.; Williams, R. Learning Internal Representation by Error Propagation. In *Parallel Distributed Processing: Explorations in the Microstructure of Cognition*; 1986; Vol. Vol. 1.

31. Al-sharhan, S.; Karray, F.; Gueaieb, W.; Basir, O. Fuzzy Entropy: A Brief Survey. In Proceedings of the 10th IEEE International Conference on Fuzzy Systems. (Cat. No.01CH37297); IEEE; Vol. 2, pp. 1135–1139.

32. Chanwimalueang, T.; Mandic, D.P. Cosine Similarity Entropy: Self-Correlation-Based Complexity Analysis of Dynamical Systems. *Entropy* **2017**, *19*.

33. Rohila, A.; Sharma, A. Phase Entropy: A New Complexity Measure for Heart Rate Variability. *Physiol. Meas.* **2019**, *40*, 105006, doi:10.1088/1361-6579/ab499e.

34. Varshavsky, R.; Gottlieb, A.; Linial, M.; Horn, D. Novel Unsupervised Feature Filtering of Biological Data. *Bioinformatics* **2006**, *22*, e507–e513, doi:10.1093/bioinformatics/btl214.

35. Velichko, A.; Belyaev, M.; Izotov, Y.; Murugappan, M.; Heidari, H. Neural Network Entropy (NNetEn): Entropy-Based EEG Signal and Chaotic Time Series Classification, Python Package for NNetEn Calculation. *Algorithms* **2023**, *16*.

36. Heidari, H.; Velichko, A.; Murugappan, M.; Chowdhury, M.E.H. Novel Techniques for Improving NNetEn Entropy Calculation for Short and Noisy Time Series. *Nonlinear Dyn.* **2023**, doi:10.1007/s11071-023-08298-w.

37. Velichko, A.; Heidari, H. A Method for Estimating the Entropy of Time Series Using Artificial Neural Networks. *Entropy* **2021**, *23*, doi:10.3390/e23111432.

38. Velichko, A.; Belyaev, M.; Wagner, M.P.; Taravat, A. Entropy Approximation by Machine Learning Regression: Application for Irregularity Evaluation of Images in Remote Sensing. *Remote Sens.* **2022**, *14*, 5983, doi:10.3390/rs14235983.

39. Guckenheimer, J.; Oliva, R.A. Chaos in the Hodgkin–Huxley Model. *SIAM J. Appl. Dyn. Syst.* **2002**, *1*, 105–114, doi:10.1137/S111111101394040.

40. González-Miranda, J.M. Complex Bifurcation Structures in the Hindmarsh–Rose Neuron Model. *Int. J. Bifurc. Chaos* **2007**, *17*, 3071–3083, doi:10.1142/S0218127407018877.

41. Kuznetsov, S.P.; Sedova, Y. V Hyperbolic Chaos in Systems Based on FitzHugh – Nagumo Model Neurons. *Regul. Chaotic Dyn.* **2018**, *23*, 458–470, doi:10.1134/S1560354718040068.

42. Nobukawa, S.; Nishimura, H.; Yamanishi, T.; Liu, J.-Q. Chaotic States Induced By Resetting Process In Izhikevich Neuron Model. *J. Artif. Intell. Soft Comput. Res.* **2015**, *5*, doi:10.1515/jaiscr-2015-0023.

43. Hindmarsh, J.L.; Rose, R.M. A Model of the Nerve Impulse Using Two First-Order Differential Equations. *Nature* **1982**, *296*, 162–164.

44. Rajagopal, K.; Khalaf, A.J.M.; Parastesh, F.; Moroz, I.; Karthikeyan, A.; Jafari, S. Dynamical Behavior and Network Analysis of an Extended Hindmarsh–Rose Neuron Model. *Nonlinear Dyn.* **2019**, *98*, doi:10.1007/s11071-019-05205-0.

45. Zheng, Q.; Shen, J.; Zhang, R.; Guan, L.; Xu, Y. Spatiotemporal Patterns in a General Networked Hindmarsh–Rose Model. *Front. Physiol.* **2022**, *13*, 936982, doi:10.3389/fphys.2022.936982.

46. Velasco Equihua, G.G.; Ramirez, J.P. Synchronization of Hindmarsh–Rose Neurons via Huygens-like Coupling. *IFAC-PapersOnLine* **2018**, *51*, 186–191, doi:https://doi.org/10.1016/j.ifacol.2018.12.115.

47. Shi, X.; Wang, Z.; Zhou, Y.; Xin, L. Synchronization of Fractional-Order Hindmarsh–Rose Neurons with Hidden Attractor via Only One Controller. *Math. Probl. Eng.* **2022**, *2022*, 3157755, doi:10.1155/2022/3157755.

48. Shilnikov, L.P.; Shilnikov, A.; Turaev, D.; Chua, L. *Methods of Qualitative Theory in Nonlinear Dynamics. Part I*.; 1998;

49. Hindmarsh, J.; Rose, R. A Model of Neuronal Bursting Using Three Coupled First Order Differential Equations. *Proc. R. Soc. Lond. B. Biol. Sci.* **1984**, *221*, 87–102, doi:10.1098/rspb.1984.0024.